Cohesive DS-PID and FQL Control Mechanisms to Enhance the Performance of the Electric Vehicle System

A. P. Siva Subramanian[1, *], B. S. Sutha[2], K. R. Aravind Britto[3]

[1]*Department of Electrical and Electronics Engineering, SSM Institute of Engineering and Technology, Dindigul, Tamil Nadu 624002, India*
[2]*Department of Electrical and Electronics Engineering, University College of Engineering Dindigul, Tamil Nadu 624709, India*
[3]*Department of Electronics and Communication Engineering, PSNA College of Engineering and Technology, Tamil Nadu 624622, India*
sivasubramanianp82@gmail.com

Abstract—**Electric Vehicles (EVs) have become more popular and attractive in recent days, due to their benefits of zero carbon emissions, cost effectiveness, reduced maintenance, and effectiveness. In which, controlling the speed of motor and proper power regulation are the important tasks for designing the EV systems. For this purpose, various control techniques have been developed in the existing works, but it limits with the major problems of reduced efficiency, increased error output, and high time consumption. To solve these problems, this paper intends to develop an advanced and novel optimization-based control algorithms for controlling the speed of motor and regulating the output power of EV systems. Here, the Maximum Peak Point Control (MPPT) technique is utilized to extract the increased amount of power from the PV panels. Then, the Dual Fold Luo (DFLuo) DC-DC converter topology is utilized to regulate the output DC power to improve the battery storage of the EV system. Consequently, the optimization-based Dynamic Supervision-PID (DS-PID) control mechanism is employed to recognize the maximum power from PV to generate the control pulses for switching activities. After that, the Fractional Quadratic Linearizer (FQL) control technique is utilized for controlling the speed of BLDC motor, in which the current limiter controls the speed based on the input features of the brake and the speed of motor running at each time instant. During the simulation evaluation, the results of the proposed control mechanisms are validated and compared using various performance measures.**

Index Terms—**Electric vehicle; Dynamic supervision-PID controller; Dual fold Luo DC-DC converter; Fractional quadratic linearizer (FQL); Solar photovoltaic system; Maximum peak point tracking (MPPT).**

I. INTRODUCTION

In the present days, the Electric Vehicle (EV) [1], [2] application has gained a significant attention due to their enormous benefits of being noiseless, having no vibration, having no smell, and the comfort of gear changes. Generally, the EV is a kind of electrically driven vehicle that can use electric motors for its impulsion. Furthermore, applications such as smart grid, EV, and other electrical

devices use solar PV system with DC-DC converters to regulate and increase the input DC voltage to the desired level [3]–[5]. Conventionally, various types of DC-DC converters have been utilized, which can be differentiated based on their design properties and the architecture of the switching arrangement. In which, the efficiency of converter topologies depends on the control of switching components present in it. Converters can reduce and boost the input power based on the arrangement of switching devices, filtering components of inductors, and capacitors. In existing works [6]–[8], closed-loop controllers have been mainly used to generate pulses in random width size according to the estimated error signal obtained from the feedback loop. To control the switches, several methods are developed to generate triggering pulses based on the feedback signal and reference parameters. Those methods [9]–[12] refer to some fixed rules with certain limits to evaluate the error signal. Since these traditional control methods are limited with the problems of reduced efficiency in regulating the power with distorted output.

To solve this problem, a novel control methodology is proposed in this work that helps to solve the fixed-range issues by estimating the control signal with respect to the varying parameters, which are dynamically updated at every time instant based on the feedback signal. This type of dynamic update will tune the performance of controller with reduced error values and regulated DC power at the output terminal. This model helps to extract the signal features for tuning the parameters of controller and, provides dynamic change in gain properties to regulate the DC power. The control signals are used to trigger the switches present in the converter circuit and the current limiter. In this case, the current limiter controls the speed of EV based on the input features of the brake and the speed of the motor running at each time instant. The main objectives of this research work are listed as follows:

– To properly regulate the maximum amount of power generated from the PV modules, the Dynamic Supervision-based PID (DS-PID) control technique is

utilized that provides the best selection of parameters based on the distance between the gain values;

− To obtain the regulated DC output power with reduced error values, the Dual Fold Luo (DFLuo) DC-DC converter topology is employed;

− To efficiently improve the control performance of EV system based on the dynamic update of parameters, the Fractional Quadratic Linearizer (FQL)-based controller design is developed;

− To validate the results of the proposed control system, various evaluation metrics have been considered during the performance analysis.

The remaining sections of this paper are structured as follows. Section II discusses the conventional converter and controller topologies used to enhance the effectiveness and performance of EV application systems. Section III presents a detailed description of the proposed methodology with its schematic representation, converter circuit topologies, and clear algorithmic illustrations. Section IV comprises the simulation and performance of the proposed control technique using various evaluation metrics. Finally, Section V summarizes the overall results of this paper with its future scope.

II. RELATED WORKS

This section investigates some of the existing works related to converter designs and control algorithms used to improve the efficiency and performance of EV systems. Also, it discusses the advantages and disadvantages of each technique based on its working principles and operating functions.

Kushwaha and Singh [13] suggested a modified Luo converter topology to improve the electric charging capability of EV systems. The main intention of this work was to minimize the computational complexity of Discontinuous Conduction Mode (DCM) selection operations with the use of a reduced number of sensors. Also, it aims to increase the power quality of the overall system at constant current voltage levels. Here, the voltage conversion ratio was computed to achieve an increased DC voltage gain. The major benefit of using this modified Luo converter-based charging system was that it efficiently controls the battery current within a certain range. Here, the dynamic performance of this system was validated under varying operating conditions. Still, the limitation of this system was cost efficiency and an increased level of harmonic contents. Faridpak, Farrokhifar, Nasiri, Alahyari, and Sadoogi [14] implemented a new converter design named the "Super-Lift Buck Converter" (SLBC) by incorporating the designs of both conventional super-lift Luo and buck converter topologies for EV application systems. The main aim of developing this converter was that it produces two step-up and step-down outputs with the single input, which helps to obtain an increased voltage gain. Also, it supports to improve the power efficiency without any additional transformer circuits. Here, the efficiency of this converter has been tested on the basis of loss factors, RMS values, and inductor currents. The benefits of the SLBC converter were a simple control model, high voltage gain, and reduced conduction loss.

Chandrasekaran, Karthikeyan, Kumar, and Kumarasamy [15] utilized dragonfly and Ant Lion Optimization (ALO) techniques to provide the appropriate solution to solve the System-on-Chip (SoC) scheduling problem with reduced cost and time consumption. Here, the clear working methodology of the dragonfly and ALO techniques with its appropriate mathematical modeling was provided. Chandrasekaran, Periyasamy, and Rajamanickam [16] suggested some Artificial Intelligence (AI)-based optimization techniques such as Ant Colony Optimization (ACO), Multi-Objective ACO (MACO), Artificial Bee Colony (BAC), Bat, and firefly to obtain fast and accurate solutions to solve the complex optimization problems. Chandrasekaran, Periyasamy, and Karthikeyan [17] recommended modified firefly and Artificial Bee Colony (ABC) optimization techniques to find the best optimal solution for SoC task scheduling with reduced cost.

Singh and Kushwaha [18] introduced an interleaved Luo converter to improve the power charging at steady state in EV system with reduced cost consumption. This converter was mainly deployed to reduce the switching conduction losses and current stress by integrating the low input and output current ripples. The key benefits of using this system were as follows: it was simple in design, reduced charging cost, andsmaller inductor size. Mehta and Haque [19] utilized an advanced Luo DC-DC converter topology to obtain the stable and ripple-free output voltage for EV systems. Typically, the Luo converter has the ability to provide reduced output ripples and parasitic effects. Hence, it was more suitable for the EV systems, which support to obtain an increased power density and lower harmonic distortions. In this paper, the main purposes and advantages of using the Luo converter for EV systems have been studied. Kamaraj and Nallaperumal [20] developed a modified multi-port Luo converter design using the voltage lift technique to improve the performance of EV systems. Here, the transient responses such as settling time and overshoot have been computed to estimate the overall behavior of the system. The state space analysis was estimated under various operating modes to efficiently regulate the load power.

Agrawal, Shrivastava, Tiwari, Ambikapathy, and Rai [21] designed an optimized control technique by selecting the converter mode to improve the quality of the power factors, considering the major factors of the reduced harmonics and the improved power factor. Also, State Space Averaging (SSA) modeling has been utilized for validating the stability of the mechanism. Kushwaha and Singh [22] utilized a flyback converter design to obtain an improved voltage gain with reduced cost consumption. The main intention of this work was to efficiently reduce the conduction loss, cost consumption, and switching voltage stress. Here, the output of the converter has been regulated with ensured supply voltage. Arumugam and Logamani [23] implemented an adaptive control mechanism with the modified Luo converter topology to improve the progression of power conversion. The main intention of this paper was to increase the gain efficiency of power transfer with reduced output ripples and induction losses. Moreover, it incorporates the functions of both flyback and Luo converter designs to attain the benefits of increased output gain, simple design, and minimal cost consumption. Deepa, Baig, Mohith, and

Abhinav [24] employed an advanced DC-DC converter topology with the state space averaging technique to obtain ripple-free voltage. The aim of this paper was to improve the voltage transfer gain of the power management system.

The authors in [25] introduced a negative output Luo converter design to improve the output voltage and power transfer efficiency of the EV system. The main intention of this converter was to efficiently control the speed of motors under varying irradiances. Then, the output of this converter was highly dependent on the parameters of current ripples, input voltage, duty ratio, and switching frequency. Here, the increased voltage gain was obtained under the continuous conduction model. During the evaluation, both the motor current and the output voltage of the converter were assessed on the basis of the varying irradiance and voltage conditions. Nachimuthu, Chinnusamy, and Mark [26] recommended a Single Ended Primary Inductor Converter (SEPIC) design to improve the power conversion efficiency and transfer capability of EV systems. The main characteristic of this converter was high step-up static gain, which helps to increase the performance of the motor with stabilized DC voltage. In this system, the high frequency transformer circuit has been utilized to step-up the input voltage without changing the frequencies. Reddy and Sudhakar [27] recommended a high-gain interleaved boost converter to improve the performance of EV systems. Here, the Radial Basis Function Network (RBFN)-based control algorithm was used to extract the maximum power from solar PV systems. Then, the interleaving technique was also utilized to reduce current ripples and voltage stress across the semiconductor devices.

Meshram, Mahajan, Kuhite, and Ujawane [28] suggested that the Brushless Direct Current (BLDC) motor improve the efficacy of EV systems, because it helps to improve the power generation efficiency of solar PV systems. In this paper, the key benefits of using a BLDC motor in EV applications have been stated, including low maintenance cost, reduced losses, and ensured energy efficiency. Kose and Muhurcu [29] deployed the chaotic-based synchronization mechanism to control the BLDC motor used in EV systems. In this model, the optimal values of the coefficients were computed using the ABC-based optimization mechanism. In addition, the performance of this control technique has been determined by the error values and stability analysis. The advantages of this work were reduced steady state error, settling, and overshoot time. Yet, it has the limitations of increased complexity in algorithm design and reduced efficiency of performance. Table I compares the conventional converter and control models for improving the voltage support grid-PV systems.

On the basis of this review, it is studied that the existing control mechanism and converter topologies are mainly used to increase the output voltage and power efficiency of EV systems. Still, it faces the major problems related to the factors of increased error rate, losses, and reduced performance results. Therefore, this research work intends to develop an advanced mechanism to improve the power quality and voltage gain of EV applications.

TABLE I. SURVEY OF VARIOUS EXISTING TECHNIQUES.

References	Methodology	Benefits	Demerits
Kushwaha and Singh [13]	Modified Luo converter topology	Battery current within certain range	Cost efficiency and increased THD
Singh and Kushwaha [18]	Interleaved Luo converter	Simple in design, reduced cost, and lower inductor size	Increased error output
Kamaraj and Nallaperumal [20]	Modified multi-port Luo converter design with voltage lift technique	Better transient response in terms of reduced peak overshoot and settling time	High THD and reduced efficiency
Agrawal, Shrivastava, Tiwari, Ambikapathy, and Rai [21]	Optimized control technique with State Space Averaging (SSA) modeling	Improved voltage gain and reduced cost consumption	Unregulated voltage output
S S, Selvan N B, and Subramaniam [25]	Negative output Luo converter design	Power transfer efficiency and increased voltage gain	High designing complexity
Nachimuthu, Chinnusamy, and Mark [26]	Single-Ended Primary Inductor Converter (SEPIC) design	Increased power conversion efficiency and stabilized DC voltage	High voltage stress and loss of power
Reddy and Sudhakar [27]	Radial Basis Function Network (RBFN)-based control algorithm	Minimized current ripples, and voltage stress	High harmonic content and increased error value
Kose and Muhurcu [29]	Chaotic-based synchronization mechanism	Reduced steady state error, minimized settling time and, overshoot time	Increased complexity and reduced efficiency

III. PROPOSED METHODOLOGY

This section presents a detailed description of the proposed methodology with clear schematic and algorithmic illustrations. The main objective of this work is to develop a new control methodology to improve the battery performance of an EV system with regulated DC output power. In addition, it is intended to control the speed of the BLDC motor used in the EV system by optimally generating the control signals. For this purpose, advanced control mechanisms such as Fractional Quadratic Linearizer (FQL) and Dynamic Supervision-based PID (DS-PID) are developed in this work. The novel contributions of using these techniques are that it estimates the control signal with respect to various parameters used for solving the fixed-range issues, and these parameters are dynamically updated at every time instant based on the feedback signal. Then, it helps to improve the performance of controller by tuning the parameters with reduced error values and regulated DC output power. The overall flow and schematic representation of the proposed system are shown in Figs. 1 and 2, respectively, which include the following stages:

− Solar PV Power Extraction;

− Power regulation using DFLuo DC-DC converter;

− DS-PID control mechanism;

− FQL-based control for the current limiter.

Initially, the maximum amount of power is extracted from

the solar PV system using the typical MPPT controller. Generally, unregulated random power can be extracted from PV panels, which is regulated to increase the output given to the EV battery. For this purpose, the DFLuo DC-DC converter topology has been utilized in this design, which helps to improve the performance of the EV system by efficiently increasing the output power. After that, the DS-PID control mechanism is mainly deployed to generate control pulses by properly recognizing the maximum PV

power. Also, it obtains the feedback signal with the parameters of the reference motor speed and torque to activate the switches. Consequently, the speed of the BLDC motor used in the EV system is controlled by using the current limiter, which helps to increase the current speed with respect to the brake input. For this purpose, the FQL-based control mechanism is implemented, which controls the speed of the EV based on the input features of the brake and the speed of the motor running at each time instant.
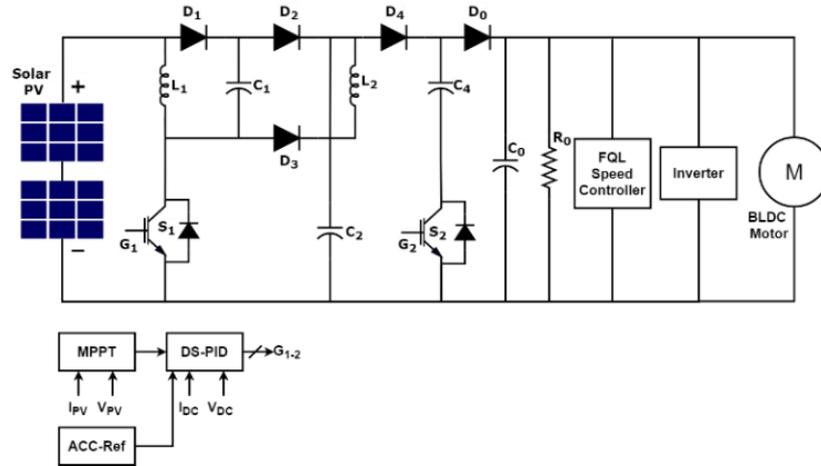

Fig. 1. Overall flow of the proposed system.

Fig. 2. Schematic representation of the proposed system.

A. Luo Converter

Typically, unregulated random power can be generated from the solar PV system by using the MPPT control technique, so it must be regulated before being given to the load system. There are different types of converter topologies that have been used to regulate the output power of the PV system. Compared to the other DC-DC converters, Luo converters are the most suitable option for boosting the output of the PV system. Because it has the major advantages of increased output voltage, reduced ripples, high density of power, and ensured efficiency. Still, it limits to the problems of high ripple voltage and reduced gain output. To solve these problems, the Dual Fold Luo (DFLuo) DC-DC converter has been utilized in this proposed system, which helps to regulate the DC output power by providing dynamic change in the gain properties. The designing properties of the proposed DFLuo converter

are given below. The selection of inductors L_1 and L_2 is derived as follows

$$L_1, L_2 = \max(d) \times \left(\frac{\min(V_{pv})}{\Delta I_0 \times f_s} \right), \qquad (1)$$

where d represents the duty cycle, ΔI_0 defines the difference in the load current, I_0 denotes the time sample, V_{pv} indicates the voltage across the PV system, and f_s is the switching frequency. Then, the current difference ΔI_0 of the load at the terminal is estimated as follows

$$\Delta I_0 = \frac{I_0(V_0 \times Th)}{\min(V_{pv})}, \qquad (2)$$

where V_0 indicates the output voltage across the load terminal, and Th is the threshold value for the ripple current

at the output terminal. In this case, the output voltage is calculated based on the duty cycle of switching activities, and is represented as follows

$$V_0 = 3V_{pv}\left(\frac{4-d}{1-d}\right). \tag{3}$$

The switching activities make the inductor electrified. Due to this, the output current is driven directly from the capacitor C_0. The input and output RMS currents of the circuit are calculated as follows:

$$I_{C_0}(RMS) = I_0\sqrt{\left(\frac{V_0 + V_D}{min(V_{pv})}\right)}, \tag{4}$$

$$I_{C_{in}}(RMS) = \frac{\Delta I_0}{\sqrt{\varphi}}, \tag{5}$$

where V_D indicates the voltage drop across diodes D_1 to D_4 and φ represents the number of switching cases. Then, the output capacitance value is estimated as follows

$$C_0 = \frac{I_0 \times d}{V_r X_\alpha X_{fs}}, \tag{6}$$

where V_r indicates the ripple voltage, X_α is the impedance value for the half cycle in d, and X_{fs} indicates the impedance value at the switching frequency. The circuit representation of the proposed DFLuo DC-DC converter is shown in Fig. 3.

Fig. 3. Schematic representation of the DFLuo DC-DC converter.

The four different operating modes (i.e., Mode 1 to Mode 4) with its switching activities are depicted from Fig. 4 to Fig. 7. In operation Mode 1, the PV current charges the inductor L_1 and flows through the switch S_1. Then, the PV current I_{PV} is subtracted with I_{L1} passes through the diode D_1, which charges the capacitor C_1, and the capacitor current I_{C1} flows through the diode D_2 and makes the capacitor C_2 charge through the switch S_1. Consequently, the capacitor C_2 current flows through the diodes D_0 and D_4 to make capacitor C_0 to get the charge up to the rated voltage. Then, this current flow of the capacitor to the load is assumed to be R_0. In this mode, the switch S_1 is in the ON state and S_2 is in the OFF state, as shown in Fig. 4.

In operation Mode 2, the PV current flows through the inductor L_1 and the diode through switch S_2, which causes the inductor L_1 to charge. Then, the inductor current L_1 flows to the capacitor C_1 to obtain charge up to the rated voltage. It also flows to the capacitor C_2 and causes it to charge through the diodes D_1 and D_2. Consequently, capacitor C_2 is discharged through diode D_4 and capacitor C_4 through switch S_2. Similar to that, the capacitor C_4 discharges through the diode D_0 and causes the capacitor C_0 to charge, and this discharge of current from C_4 flows through the load. In this mode, the switch S_1 is in the OFF state and S_2 is in the ON state, as shown in Fig. 5.
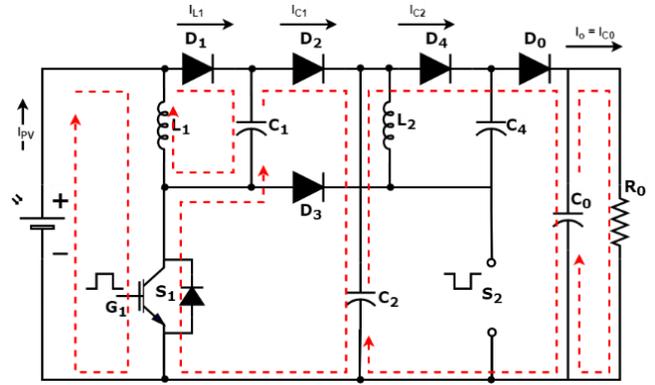

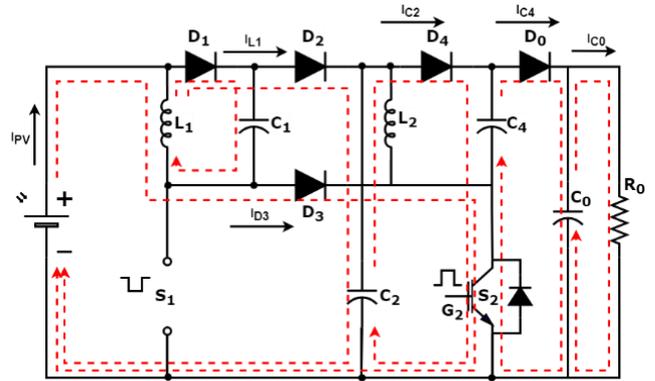Fig. 4. Operation Mode 1 (S_1 ON and S_2 OFF).

Fig. 5. Operation Mode 2 (S_1 OFF and S_2 ON).

In operation Mode 3, both switches S_1 and S_2 are in the ON state, where the PV current flows through the inductor L_1 and switch S_1, and this current also flows through the diode D_3 and capacitor C_2, which is depicted in Fig. 6. The charging of current in the inductor charges the capacitor C_1 to get charge through the diode D_1. The discharge current from C_1 flows through the inductor L_2 through diode D_2. The capacitor current C_2 discharges through the capacitor C_4 and switch S_2. At the terminal of capacitor C_4, the current C_2 and L_2 are added to charge capacitor C_4. This current flow from C_4 charges the capacitor C_0 up to the rated power and is passed to the load.

The operation Mode 4 fully acts with the discharging current of the capacitor and the inductor, where both switches are turned OFF. The current from PV passes through the inductor L_1 and diode D_3 to charge the capacitor C_2 and the inductor L_1. The discharge current of L_1 flows through the diode D_1 and capacitor C_1. The charged inductor L_2 started to discharge through the capacitor C_4 and circulate internally. The discharge of current from C_2 flows through the diode D_4 and D_0 to charge the capacitor C_0. The current discharge from capacitor C_0 passed through the load. The waveform patterns of these switching activities are shown in Fig. 8, where the pulses are given to the switches with the
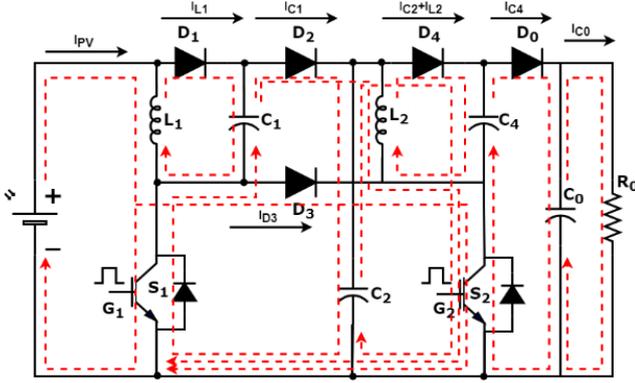
amplitude of volts.
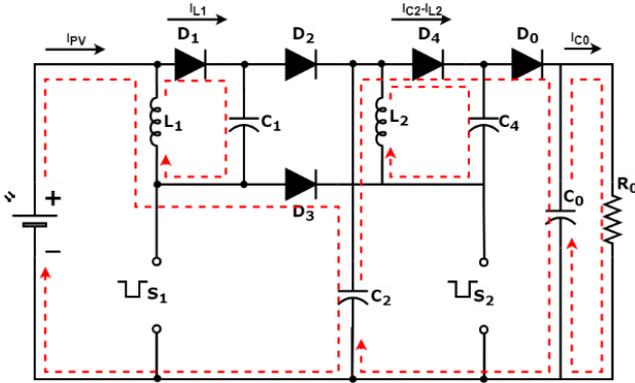

Fig. 6. Operation Mode 3 (S_1 ON and S_2 ON).

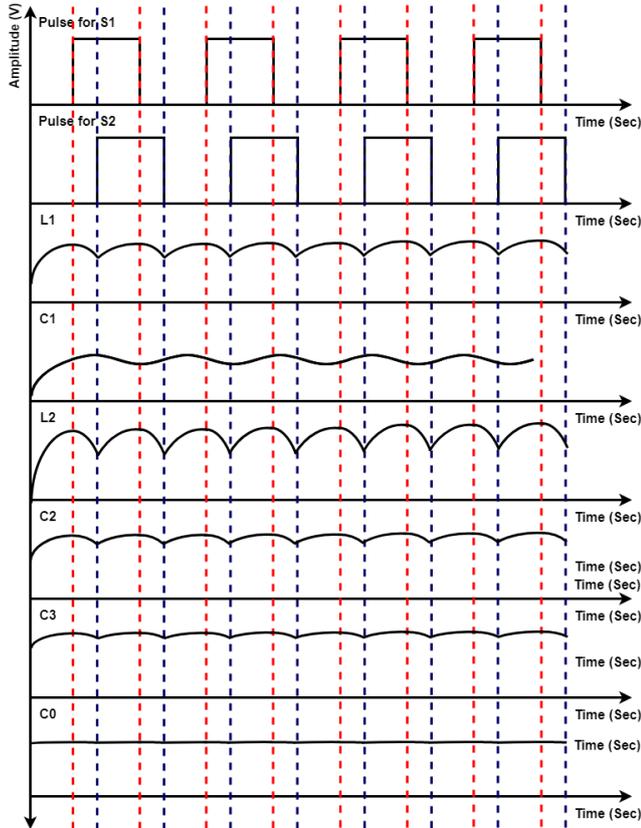Fig. 7. Operation Mode 4 (S_1 OFF and S_2 OFF).

Fig. 8. Waveform pattern of switching activities.

B. DS-PID (Dynamic Supervision-based PID) Optimal Controller

In this work, the DS-PID based optimized control technique is mainly developed for recognizing the maximum amount of PV power to generate the controlling pulses. Typically, PID control techniques are widely used in EV application systems due to their benefits of increased robustness, high efficiency, and simple design. However, the control performance of this technique is not efficient, and it results in a long delay in the process. Therefore, the proposed work intends to develop an optimization-based PID control technique for proper power recognition. In this technique, the duty cycle converter parameters, the switching frequency, and the error signal are considered as input for processing, and it produces the best selection of parameters, such as K_p and K_i are the outputs.

At first, the gain parameters such as K and K_{max} are initialized with the search limits of $K_p(max)$ and $K_i(max)$. Here, the Euclidean distance D is computed between the predicted and previous values with respect to the gain parameters as shown below

$$D = \left| C \times X^*(i) - X(i) \right|, \tag{7}$$

where X represents the optimization particles at the current position, X^* is the optimization particles of at the previous position, and C denotes the coefficient value of the particles X. Based on this distance value, the next position of particles is computed as follows

$$X(i+1) = X^*(i) - A \times D, \tag{8}$$

where A indicates the coefficient of particles at the next iteration point. Consequently, the coefficient values of A and C are estimated based on the following equations:

$$A = 2ar - a, \tag{9}$$
$$C = 2r, \tag{10}$$

where a indicates the convergence value from max to 0, and r is the arbitrary variable (Boundary parameter) ranging from 0 to 1. Then, the objective function of the optimization is computed as follows

$$F(d) = \frac{\sum X}{max(X)}. \tag{11}$$

If the value of $F(d)$ is greater than 0.5, then the value of d can be increased by 0.1 and the following condition is verified

$$d_{min} \leq d \leq d_{max}. \tag{12}$$

After that, the next instant of duty cycle is estimated as shown below

$$d(i+1) = d(i) - A \times D. \tag{13}$$

Consequently, the convergence has been verified once, and, based on this condition, the parameters are optimally selected with the duty cycles as illustrated as follows:

$$K'_p = K_p(d), \tag{14}$$
$$K'_i = K_i(d). \tag{15}$$

Finally, the switching pulses are generated according to the duty cycle of d' with the best selection of parameters. Furthermore, it is used to check whether the DC power input meets a certain limit based on the accelerator reference value. The detailed algorithmic illustration of the proposed DS-PID control technique is shown below (Algorithm 1).

Algorithm 1. DS-PID Optimized Control Mechanism.

Input: Converter Parameters (Duty cycle, switching frequency and error signal)
Output: Best Selection of K_p, and K_i
Step 1: Initialize gain parameters K and K_{max} and search boundaries K_p(max) and K_i(max).
Step 2: Let "D" be the Euclidean distance between the predicted and the previous value of the gain parameters. It is estimated using (7) with respect to the parameters of the optimization particles at the current position, the optimization particles at the previous position, and the coefficient value of the particles.
Step 3: From this distance, the next position of the particles is calculated using (8) based on the coefficient of particles at the next iteration point.
Step 4: These coefficient values "A" and "C" can be calculated using (9) and (10), respectively.
Step 5: The objective function of optimization can be defined using (11).
Step 6: If F(d) > 0.5, then
    Increase "d" with 0.1.
    Check whether $d_{min} \leq d \leq d_{max}$.
End if
Step 7: Estimate the next instant of duty cycle as shown in (13);
Check for convergence.
If $F(d)^{i+1} < F(d)^i$, then
    $d' = d(i+1)$
Else
    $d' = d(i)$
End if;
Step 8: Select K_p and K_i as represented in (14) and (15), respectively;
Step 9: Generate the pulse according to d'.

C. Fractional Quadratic Linearizer (FQL) Controller

In this work, the main intention of using the Fractional Quadratic Linearized (FQL) control technique is to control the speed of the motor used in the EV system. The novel contribution of this technique is that it efficiently extracts the signal features for tuning the controller parameters with the current limiter unit. Here, the control signals are used to trigger the switches present in the converter circuit and the current limiter. This type of current limiter controls the speed of vehicle based on the input features of the brake and speed of motor running at each instant of time. In addition, this mechanism helps to increase the stability of the system by improving the voltage quality with reduced error values. Moreover, it controls the motor speed by analyzing the control signals obtained from the DS-PID mechanism, the output of the motor driving component, and the brake input. On the basis of these, the current limiter predicts the limit of current for controlling and maintaining the speed of BLDC motor used in the EV system. In this technique, the acceleration reference, BLDC motor parameters, DC voltage, and current are obtained as input, and the current value provided to the BLDC motor is produced as output, which helps to control the speed of EV. In which, the control parameters such as $\beta, \gamma, \rho, \lambda$, and μ are initialized at first, and the objective function of this control algorithm is

computed as follows

$$f_{obj} = \sqrt{\sum_{i=0}^{T} \frac{(N(t)_{Ref(i)} - N(t)_{est(i)})^2}{T}}, \qquad (16)$$

where $N(t)_{Ref(i)}$ indicates the reference speed at each time instant t, and $N(t)_{est(i)}$ represents the estimated speed at each time instant t. Based on this function, the minimum values of the control parameters are calculated with respect to the current flow given to the motor. The detailed algorithmic steps involved in this mechanism are represented as follows (see Algorithm 2).

Algorithm 2. FQL algorithm.

Input: Acceleration reference, BLDC parameters, and the DC voltage and current
Output: Current value of the BLDC motor (Control the speed of the vehicle).
Step 1: Initialize controller parameters $\beta, \gamma, \rho, \lambda$, and μ
Step 2: The objective function of the algorithm can be represented using (16) with respect to the reference speed and the estimated speed at each time instant.
Step 3: If $f_{obj} > f'_{obj}$, then
    Update the controller parameters.
Calculate change of current to motor.
End if
Step 4: Select the minimum values of $\beta, \gamma, \rho, \lambda$, and μ parameters.
Step 5: Update the current flow to the motor.

The major advantages of the proposed control DS-PID incorporated FQL control mechanism are as follows:
− High regulated DC output power;
− Proper recognition of PV power;
− Efficient current control based on the current limit;
− Increased motor speed with respect to load power, current;
− Ensured system stability and reliability.

IV. RESULTS AND DISCUSSION

This section presents the simulation and performance analysis of the proposed DS-PID with FQL control mechanisms used in the EV system. Here, the simulation is performed by using the MATLAB/SIMULINK tool that supports to implement and validate the results of the proposed work. Also, the proposed control schemes are validated by extracting the scope at varying points of the circuit in both inverter and converter blocks. Moreover, this setup has been presented with the use of logical components and design blocks available in the Simulink. Then, it is used to take the intermediate results with the waveforms displayed in the Simulink scope. The results of both existing and proposed mechanisms are validated by using different performance measures such as IV and PV characteristics of the PV system, speed of the BLDC motor, capacitor current, DC current, DC voltage, gate pulses, inductor current, motor current, step response, Total Harmonics Distortion (THD), and voltage across the capacitor. In addition to that, some of the existing optimization-based control mechanisms are compared with the proposed technique with respect to the parameters of Integral Square Error (ISE), Integral Absolute Error (IAE), Integral Time Absolute Error (ITAE), and Integral Time Square Error (ITSE).

A. Simulation Analysis

Generally, the IV and PV characteristics of the solar PV system are validated with respect to the obtained current and power values, as shown in Fig. 9(a) and Fig. 9(b), respectively. In this analysis, the IV and PV characteristics are estimated under varying voltage levels ranging from 0 V to 25 V. Typically, the performance of the MPPT control technique used to extract the maximum amount of power from the PV panels is validated on the basis of these IV and PV characteristics. In addition, the reliability and accuracy of the PV power extraction system is highly dependent on these measures. In the proposed work, the DFLuo converter topology has been utilized to boost the output power obtained from the PV panels, which helps to efficiently increase the output voltage and power.

Fig. 9. (a) IV characteristics; (b) PV characteristics.

Figure 10 shows the speed of the BLDC motor with respect to the varying time values in terms of seconds, where the speed is estimated in RPM. Generally, the speed of the motor has been controlled on the basis of the parameters of input DC voltage and current. For this purpose, the DS-PID and FQL optimization-based control mechanisms are deployed in this system, which efficiently controls the speed of the motor based on the current limiter. Here, the speed has been maintained in the range of 1000 RPM at 0.1 s by optimally controlling the parameters with respect to the acceleration speed.

Figure 11 shows the capacitor C_0 current in terms of Amps under varying time samples ranging from 0 to 600. Normally, the capacitors used in EV systems help to reduce the ripple current and the regulated DC bus voltage. In this evaluation, the current across the capacitor C_0 has been analyzed at different time instances, where it is saturated in the range of 35 A. Similarly, to that, the DC current is also

estimated under varying time samples, as shown in Fig. 12. It is mainly used for charging the batteries of EV system, where it is saturated with 60 A at 300 time samples.
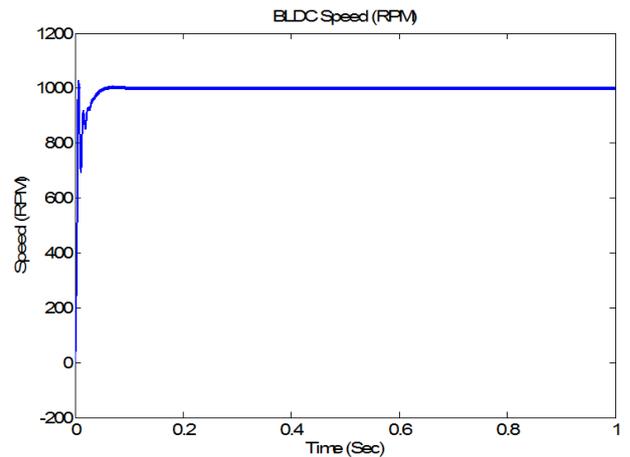
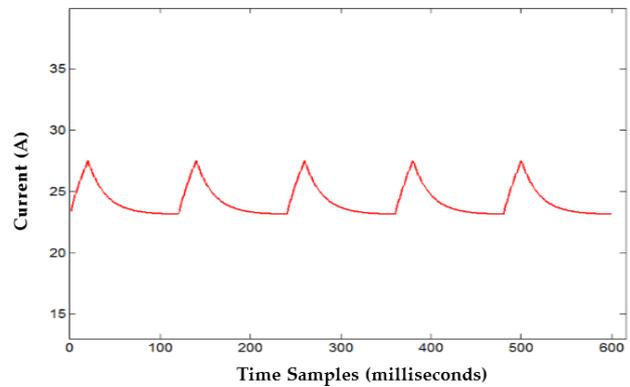

Fig. 10. Speed of the BLDC Motor.
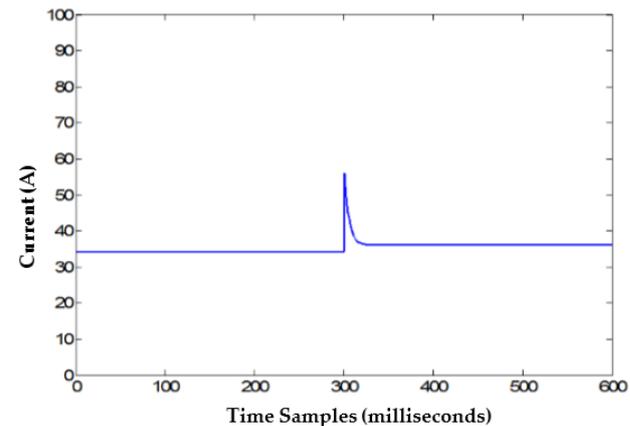

Fig. 11. Current of the Capacitor C_0.

Fig. 12. DC Current.

Figure 13 shows the DC voltage under varying time samples ranging from 0 to 600, which shows that continuous DC supply has been provided to the BLDC motor of the EV system to manage and control the speed at the constant rate. Figure 14 illustrates the gate pulses generated by the control technique with respect to varying time (s). On the basis of the transfer function of the control mechanism, the control signal has been provided to the gates for generating the pulses. Figure 15 represents the inductor L_1 current (A) under varying time samples, which is estimated by the inductor current provided to the DFLuo converter. Consequently, the current of the BLDC motor is validated

with respect to different time samples, as shown in Fig. 16. Based on the feedback signal and converter output, the controller can generate the optimized control signals to regulate both the output of the DC and the motor current of the inverter.
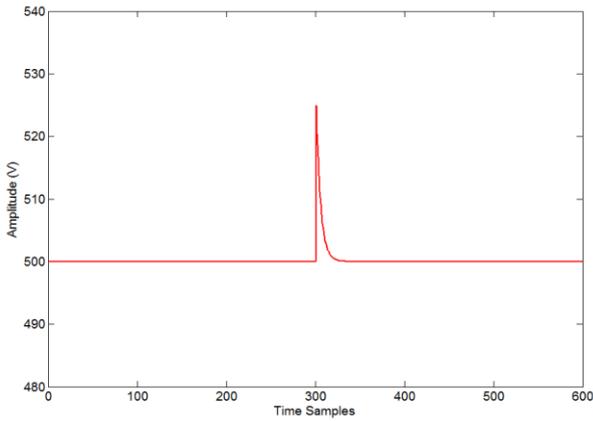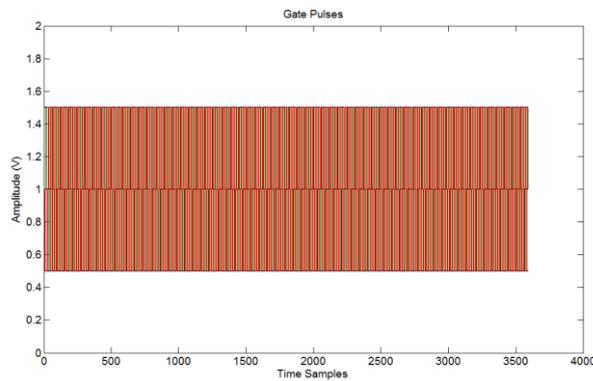
Here, the controller can generate the control signals to activate the gates switches based on the optimized transfer function. In the output terminal, the response of controller has been validated at the sudden change, which is termed the step response of controller, which is shown in Fig. 17.

Fig. 13. DC Voltage.

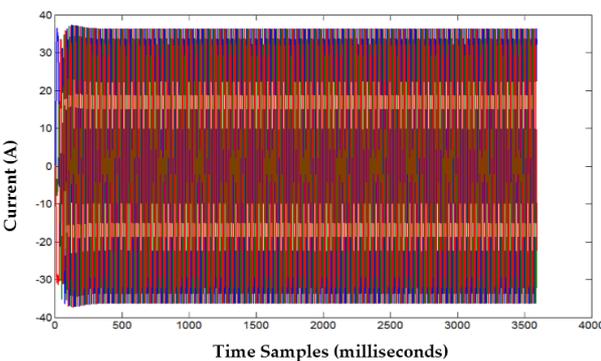Fig. 14. Gate Pulses.

Fig. 15. Current of the L_1 Inductor .
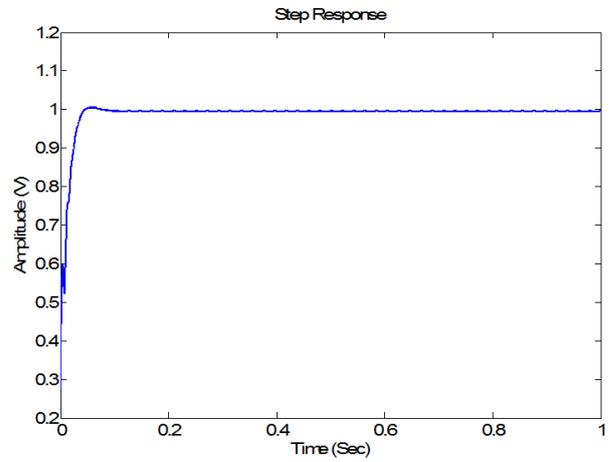

Fig. 16. Motor current I_{abc}.

Fig. 17. Step response.

The proposed DS-PID and FQL control techniques increase the gain value of output power with reduced harmonics. Then, it can be validated at varying frequency ranges (Hz) and magnitude of fundamental (50 Hz), as shown in Fig. 18.
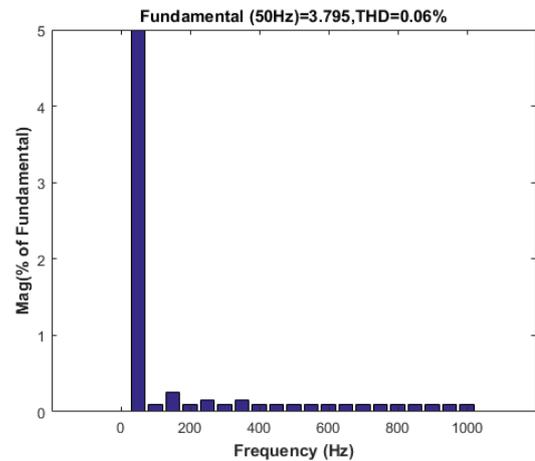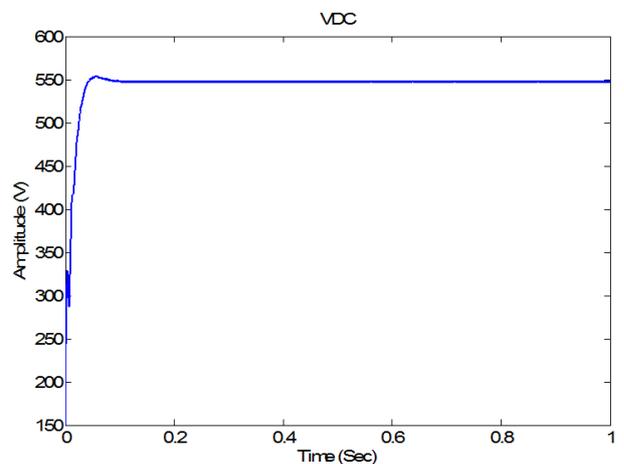

Fig. 18. THD analysis.

Fig. 19. Voltage across the capacitor C_0.

From the analysis, it is evident that the lower level of harmonics ensure the improved system performance. Here, the THD has been reduced up to 0.8 % at the fundamental frequency of 50 Hz, which indicates that a lower level of harmonics exists in the AC output of the signal. The output voltage across the capacitor C_0 is shown in Fig. 19 with respect to the varying time instances (s). This result shows that the V_{DC} has been maintained at the constant level under varying time instances, which proves the effectiveness of the converter topology.

B. Comparative Analysis

To prove the efficiency of proposed DS-PID and FQL control techniques, they are compared with some state-of-the-art [30], [31] optimization-based control techniques based on different evaluation metrics. Figure 20 and Table II show the comparative analysis of existing and proposed optimization-based control techniques with respect to the measures of rise time, peak time, settling time, peak overshoot, ISE, and IAE. Typically, the PID control technique used for the BLDC motor system is more cost effective. Hence, various optimization-based control techniques have been developed in the existing works, which helps to improve the speed of motor based on the optimized control function. Here, conventional Particle Swarm Optimization (PSO) and Grey Wolf Optimization (GWO) techniques have been compared with the proposed DS-PID and FQL techniques. In this case, the rise time is defined as the amount of time taken by the plant to rise the output at the desired level for the first time. Then, the settling time is estimated based on the amount of time that the system goes to the steady state. Moreover, the peak time is defined as the amount of time taken by the controller to produce the maximum power output. Compared to these techniques, the proposed DS-PID- and FQL-based control mechanisms require a reduced time consumption in terms of seconds, which shows the effectiveness of the proposed scheme.
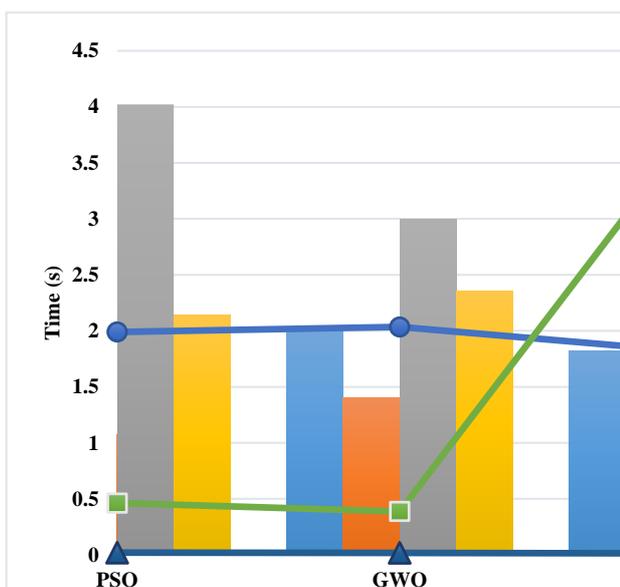

Fig. 20. Comparative analysis of existing and proposed optimization-based control techniques.

TABLE II. ANALYSIS OF RISE TIME, PEAK TIME, AND SETTLING TIME (s).

Algorithms	Rise Time (s)	Peak Time (s)	Settling Time (s)
PSO	1.99	1.075	4.022
GWO	2.035	1.4	3
Proposed	1.82	1.02	1.57

As shown in Table III, the peak overshoot of both existing and proposed optimization-based control techniques is evaluated at varying RPMs such as 1000 and 1500. Generally, the peak overshoot is estimated on the basis of the deviance of peak value and response time. This analysis also shows that the proposed control technique outperforms the other techniques with reduced peak overshoot at different RPM.

TABLE III. PEAK OVERSHOOT AT 1000 RPM AND 1500 RPM.

Algorithms	Peak Overshoot @ 1000 RPM (%)	Peak Overshoot @ 1500 RPM (%)
PSO	2.14	1.99
GWO	2.36	2.035
Proposed	2.05	1.82

Table IV shows the values of the Integral Square Error (ISE) and Integral Absolute Error (IAE) of both existing and proposed control techniques. Similarly, the values of the Integral Time Absolute Error (ITAE) and Integral Time Square Error (ITSE) of both existing and proposed techniques are validated and compared in Table V. These error values are mainly estimated to determine the stability of the system, and the reduced values of these measures ensure the improved performance of the system. Based on this analysis, it is evident that the proposed control mechanism outperforms the other techniques with reduced error values of these measures.

TABLE IV. ISE AND IAE OF EXISTING AND PROPOSED CONTROL TECHNIQUES.

Algorithms	ISE	IAE
PSO	1233	53.43
GWO	1035	46.86
Proposed	9843	33.75

TABLE V. ITAE AND ITSE OF EXISTING AND PROPOSED CONTROL TECHNIQUES.

Algorithms	ITAE	ITSE
PSO	1293	696.9
GWO	915.9	489.6
Proposed	847.3	364.7

Figure 21 shows comparative analysis of existing and proposed optimization-based control techniques based on ITAE and ITSE.

Figure 22 and Table VI compare existing and proposed optimization-based control techniques with respect to the parameters of rise time (s), peak time (s), and maximum speed (rpm). Compared with these techniques, the proposed DS-PID integrated with FQL control techniques provides improved performance results with reduced values of these parameters. This is so because, in the proposed scheme, the signal features are efficiently extracted to tune the controller parameters, providing the dynamic change in gain properties with regulated output power.
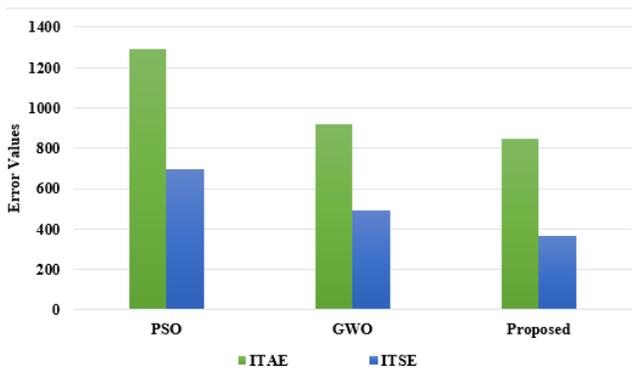
Fig. 21. Comparative analysis of existing and proposed optimization-based control techniques based on ITAE and ITSE.
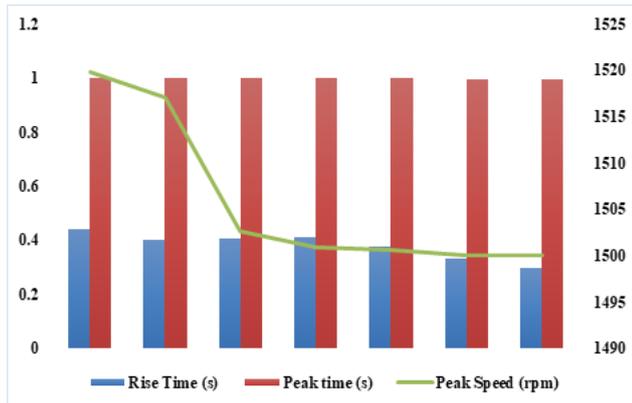

Fig. 22. Comparative analysis between existing and proposed techniques based on the rise time, peak time, and peak speed.

TABLE VI. RISE TIME, PEAK TIME, AND PEAK SPEED OF EXISTING AND PROPOSED CONTROL TECHNIQUES.

Controllers	Rise Time (s)	Peak time (s)	Peak Speed (rpm)
Anti-windup PID	0.4391	0.9987	1519.8
Sreeram approach of FLC	0.4024	0.9989	1517.1
Neuro-Fuzzy	0.4069	0.9981	1502.7
Bat Algorithm	0.412	1.0009	1501
Flower Pollination Algorithm	0.3785	1.0007	1500.7
New SMA-WNL-Type 2 Sugeno Fuzzy PID Controller	0.3351	0.9971	1500
Proposed	0.2983	0.9957	1500

Figure 23 and Table VII compare the existing and proposed optimization-based control techniques with respect to the parameters of peak overshoot (%), settling time (s), and steady state error (%). From these evaluations, it is observed that the DS-PID and FQL control techniques could efficiently reduce the time consumption, overshoot, and error values by optimally tuning the control parameters. Then, the results obtained are improved over the conventional techniques, which shows the overall effectiveness of the proposed scheme.

Here, the sensitivity analysis is carried out to test the performance and efficiency of Luo converter with DS-PID control technique. Normally, the sensitivity of power conversion systems is highly dependent on the output voltage gain, current, and power. Table VIII shows the voltage gain of both existing and proposed control techniques, and the obtained results depict that the proposed DS-PID with Luo converter topology gives the maximum

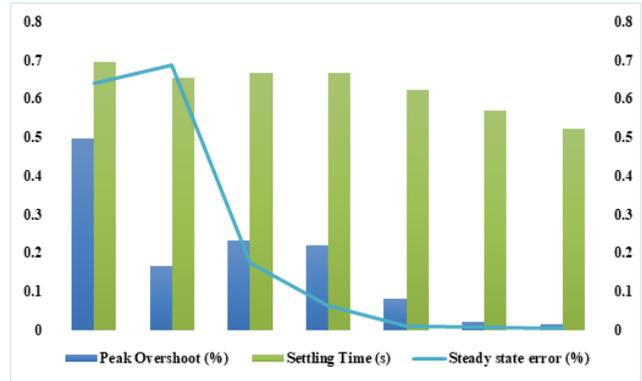gain value, when compared to other methodologies.

Fig. 23. Comparative analysis between existing and proposed techniques based on peak overshoot, settling time, and steady state error.

TABLE VII. PEAK OVERSHOOT, SETTLING TIME, AND STEADY STATE ERROR OF EXISTING AND PROPOSED CONTROL TECHNIQUES.

Controllers	Peak Overshoot (%)	Settling Time (s)	Steady state error (%)
Anti-windup PID	0.4963	0.6958	0.6391
Sreeram approach of FLC	0.1654	0.6549	0.6887
Neuro-Fuzzy	0.2334	0.669	0.1749
Bat Algorithm	0.22	0.6671	0.0647
Flower Pollination Algorithm	0.0792	0.6243	0.01
New SMA-WNL-Type 2 Sugeno Fuzzy PID Controller	0.0216	0.5695	0.0061
Proposed	0.0146	0.5227	0.00316

TABLE VIII. PEAK OVERSHOOT, SETTLING TIME, AND STEADY STATE ERROR OF EXISTING AND PROPOSED CONTROL TECHNIQUES.

Methods	Voltage gain (V)
High-gain converters	14 V
Quasi Z-Source	12 V
Interleaved	13.5 V
Proposed DS-PID and FQL	25 V

V. CONCLUSIONS

This paper presents advanced optimization control mechanisms named "DS-PID" and "FQL" to properly recognize the maximum power of the PV and control the speed of the BLDC motor used in the EV system. The novel contribution of these methodologies is that they optimally tune the para for generating the control signals to activate the switches. In addition, they dynamically update the parameters at every time instant based on the feedback signal. Here, the DFLuo DC-DC converter has been utilized to boost the output power of PV systems based on the dynamic change in gain properties. Then, the optimization-based DS-PID control technique is utilized to recognize the PV power to generate the control signals. It considers the duty cycle converter parameters, switching frequency, and error signal as input for processing, and provides the best selection of parameters for generating the control signals. Furthermore, these signals are used to trigger the switches present in the converter circuit and current limiter. This type of current limiter controls the speed of the vehicle based on the input features of the brake and the speed of the motor running at each instant of time, which is done by using the FQL-based control mechanism. During performance

analysis, the results of both existing and proposed techniques are validated and compared using various measures. From the evaluation, it is evident that the proposed control mechanism outperforms the other techniques with improved performance results. Using this control technique, the rise time is reduced to 1.82 s, the peak time is minimized to 1.02 s, and the settling time is 1.257 s. Similar to that, the steady state error is also minimized up to 0.00316 % with the peak overshoot of 0.0146 %. Consequently, the error rate of the proposed control technique is efficiently reduced, including the error rates of ISE, IAE, ITAE, and ITSE with values of 984, 33.75, 847.3, and 364.7, respectively. The results obtained show the overall efficiency and improved performance of the proposed control technique over the other techniques. Still, the proposed work is required to minimize the output ripples of the converter, and it also faces the difficulties in operating under extreme duty ratios.

CONFLICTS OF INTEREST

The authors declare that they have no conflicts of interest.

REFERENCES

[1] S. Kumaravel, R. A. Narayanankutty, V. S. Rao, and A. Sankar, "Dual input–dual output DC–DC converter for solar PV/battery/ultra-capacitor powered electric vehicle application", *IET Power Electronics*, vol. 12, no. 13, pp. 3351–3358, 2019. DOI: 10.1049/iet-pel.2019.0123.

[2] R. Sreejith and B. Singh, "Intelligent nonlinear sensorless predictive field oriented control of PMSM drive for three wheeler hybrid solar PV-battery electric vehicle", in *Proc. of 2019 IEEE Transportation Electrification Conference and Expo (ITEC)*, 2019 pp. 1–6. DOI: 10.1109/ITEC.2019.8790458.

[3] K. S. Kavin and P. Subha Karuvelam, "PV-based grid interactive PMBLDC electric vehicle with high gain interleaved DC-DC SEPIC Converter", *IETE Journal of Research*, pp. 1–15, 2021. DOI: 10.1080/03772063.2021.1958070.

[4] J. Saeed, M. Niakinezhad, L. Wang, and N. Fetnando, "An integrated charger with hybrid power source using PV array for EV application", in *Proc. of 2019 IEEE 13th International Conference on Compatibility, Power Electronics and Power Engineering (CPE-POWERENG)*, 2019, pp. 1–6. DOI: 10.1109/CPE.2019.8862426.

[5] K. V. and B. Singh, "Single current sensor-based vector control of solar PV-battery assisted induction motor drive for electric vehicle", in *Proc. of 2020 3rd International Conference on Energy, Power and Environment: Towards Clean Energy Technologies*, 2021 pp. 1–6. DOI: 10.1109/ICEPE50861.2021.9404532.

[6] R. Sreejith and B. Singh, "Position sensorless PMSM drive for solar PV-battery light electric vehicle with regenerative braking capability", in *Proc. of. 2020 IEEE Energy Conversion Congress and Exposition (ECCE)*, 2020, pp. 1447–1452. DOI: 10.1109/ECCE44975.2020.9236086.

[7] D. Andriukaitis, A. Laucka, A. Valinevicius, M. Zilys, V. Markevicius, D. Navikas, R. Sotner, J. Petrzela, J. Jerabek, N. Herencsar, and D. Klimenta, "Research of the Operator's Advisory System Based on Fuzzy Logic for Pelletizing Equipment," *Symmetry*, vol. 11, no. 11, p. 1396, Nov. 2019. DOI: 10.3390/sym11111396.

[8] D. Kumar and A. U. Ahmad, "Design an electric vehicle using PV array with five-phase permanent magnet synchronous motor", *International Journal of Trend in Scientific Research and Development (IJTSRD)*, vol. 3, no. 6, pp. 581–587, 2019.

[9] Y. Zhang, J. He, and D. M. Ionel, "Modeling and control of a multiport converter based EV charging station with PV and battery", in *Proc. of 2019 IEEE Transportation Electrification Conference and Expo (ITEC)*, 2019, pp. 1–5. DOI: 10.1109/ITEC.2019.8790632.

[10] J. Thankachan and S. P. Singh, "Solar powered high performance switched reluctance motor for EV applications", in *Proc. of 2017 IEEE 15th International Conference on Industrial Informatics (INDIN)*, 2017, pp. 389–395. DOI: 10.1109/INDIN.2017.8104803.

[11] G. Pancholi, D. K. Yadav, and L. Chaturvedi, "Energy management strategies for hybrid electric vehicle using PV, ultracapacitor and battery", in *Proc. of 2017 IEEE Transportation Electrification Conference (ITEC-India)*, 2017, pp. 1–5. DOI: 10.1109/ITEC-India.2017.8333886.

[12] A. Tavakoli, S. Saha, M. T. Arif, M. E. Haque, N. Mendis, and A. M. T. Oo, "Impacts of grid integration of solar PV and electric vehicle on grid stability, power quality and energy economics: A review", *IET Energy Systems Integration*, vol. 2, no. 3, pp. 243–260, 2020. DOI: 10.1049/iet-esi.2019.0047.

[13] R. Kushwaha and B. Singh, "A modified Luo converter-based electric vehicle battery charger with power quality improvement", *IEEE Transactions on Transportation Electrification*, vol. 5, no. 4, pp. 1087–1096, 2019. DOI: 10.1109/TTE.2019.2952089.

[14] B. Faridpak, M. Farrokhifar, M. Nasiri, A. Alahyari, and N. Sadoogi, "Developing a super-lift luo-converter with integration of buck converters for electric vehicle applications", *CSEE Journal of Power and Energy Systems*, vol. 7, no. 4, pp. 811–820, 2021. DOI: 10.17775/CSEEJPES.2020.01880.

[15] G. Chandrasekaran, P. R. Karthikeyan, N. S. Kumar, and V. Kumarasamy, "Test scheduling of system-on-chip using dragonfly and ant lion optimization algorithms", *Journal of Intelligent & Fuzzy Systems*, vol. 40, no. 3, pp. 4905–4917, 2021. DOI: 10.3233/JIFS-201691.

[16] G. Chandrasekaran, S. Periyasamy, and K. P. Rajamanickam, "Minimization of test time in system on chip using artificial intelligence-based test scheduling techniques", *Neural Computing and Applications*, vol. 32, no. 9, pp. 5303–5312, 2020. DOI: 10.1007/s00521-019-04039-6.

[17] G. Chandrasekaran, S. Periyasamy, and P. R. Karthikeyan, "Test scheduling for system on chip using modified firefly and modified ABC algorithms", *SN Applied Sciences*, vol. 1, no. 9, p. 1079, 2019. DOI: 10.1007/s42452-019-1116-x.

[18] B. Singh and R. Kushwaha, "Power factor preregulation in interleaved Luo converter-fed electric vehicle battery charger", *IEEE Transactions on Industry Applications*, vol. 57, no. 3, pp. 2870–2882, 2021. DOI: 10.1109/TIA.2021.3061964.

[19] N. D. Mehta and A. M. Haque, "Design and simulation of Luo converter for DC motor control for an electric vehicle applications", in *Proc. of International Conference on Emerging Technologies in Engineering, Biomedical, Medical and Science (ETEBMS - July 2017)*, 2017, pp. 57–61.

[20] V. Kamaraj and C. Nallaperumal, "Modified multiport Luo converter integrated with renewable energy sources for electric vehicle applications", *Circuit World*, vol. 46, no. 2, pp. 125–135, 2020. DOI: 10.1108/CW-08-2019-0104.

[21] A. Agrawal, A. Shrivastava, S. Tiwari, A. Ambikapathy, and A. Rai, "Performance analysis of Luo converter in continuous conduction mode (CCM) for electric vehicle", *AIP Conference Proceedings*, vol. 2294, no. 1, p. 040015, 2020. DOI: 10.1063/5.0031797.

[22] R. Kushwaha and B. Singh, "An improved power factor Luo converter based battery charger for electric vehicle", in *Proc. of 2020 IEEE Transportation Electrification Conference & Expo (ITEC)*, 2020, pp. 723–728. DOI: 10.1109/ITEC48692.2020.9161736.

[23] S. Arumugam and P. Logamani, "Modeling and adaptive control of modified LUO converter", *Microprocessors and Microsystems*, vol. 71, art. 102889, 2019. DOI: 10.1016/j.micpro.2019.102889.

[24] K. Deepa, Md. F. Baig, P. Mohith, and A. V. Abhinav, "Dynamic analysis of LUO converter with all parasitics", in *Proc. of 2017 International Conference on Trends in Electronics and Informatics (ICEI)*, 2017, pp. 1024–1028. DOI: 10.1109/ICOEI.2017.8300862.

[25] D. S. S, M. Selvan N B, and U. Subramaniam, "Power conditioning of standalone Photo-voltaic system with BLDC motor by Negative-Output Luo Converter", in *Proc. of 2020 International Conference on Power Electronics and Renewable Energy Applications (PEREA)*, 2020, pp. 1–6. DOI: 10.1109/PEREA51218.2020.9339815.

[26] S. Natchimuthu, M. Chinnusamy, and A. P. Mark, "Experimental investigation of PV based modified SEPIC converter fed hybrid electric vehicle (PV-HEV)", *International Journal of Circuit Theory and Applications*, vol. 48, no. 6, pp. 980–996, 2020. DOI: 10.1002/cta.2766.

[27] K. J. Reddy and N. Sudhakar, "High voltage gain interleaved boost converter with neural network based MPPT controller for fuel cell based electric vehicle applications", *IEEE Access*, vol. 6, pp. 3899–3908, 2018. DOI: 10.1109/ACCESS.2017.2785832.

[28] P. Meshram, P. Mahajan, T. Kuhite, and R. Ujawane, "Solar powered brushless Dc (Bldc) motor driven electric vehicle", *Journal of Advances in Electrical Devices*, vol. 4, no. 1, pp. 16–20, 2019. DOI: 10.5281/zenodo.2605130.

[29] E. Kose and A. Muhurcu, "The control of brushless DC motor for electric vehicle by using chaotic synchronization method", *Studies in Informatics and Control*, vol. 27, no. 4, pp. 403–412, 2018. DOI: 10.24846/v27i4y201804.

[30] A. Karuppannan and M. Muthusamy, "Wavelet neural learning-based type-2 fuzzy PID controller for speed regulation in BLDC motor", *Neural Computing and Applications*, vol. 33, pp. 13481–13503, 2021. DOI: 10.1007/s00521-021-05971-2.

[31] P. Dutta and S. K. Nayak, "Grey wolf optimizer based PID controller for speed control of BLDC motor", *Journal of Electrical Engineering & Technology*, vol. 16, no. 2, pp. 955–961, 2021. DOI: 10.1007/s42835-021-00660-5.